

# Fast Reconstruction and Data Scouting

Javier Duarte<sup>1,\*</sup>

<sup>1</sup>Fermi National Accelerator Laboratory

**Abstract.** Data scouting, introduced by CMS in 2011, is the use of specialized data streams based on reduced event content, enabling LHC experiments to record unprecedented numbers of proton-proton collision events that would otherwise be rejected by the usual filters. These streams were created to maintain sensitivity to new light resonances decaying to jets or muons, while requiring minimal online and offline resources, and taking advantage of the fast and accurate online reconstruction algorithms of the high-level trigger. The viability of this technique was demonstrated by CMS in 2012, when  $18.8 \text{ fb}^{-1}$  of collision data at  $\sqrt{s} = 8 \text{ TeV}$  were collected and analyzed. For LHC Run 2, CMS, ATLAS, and LHCb implemented or expanded similar reduced-content data streams, promoting the concept to an essential and flexible discovery tool for the LHC.

## 1 Introduction

The Large Hadron Collider (LHC) provides proton-proton bunch crossings with a center-of-mass energy  $\sqrt{s} = 13 \text{ TeV}$  at a maximum rate of 40 MHz. As such, the digital readout of the LHC detectors generate an enormous amount of raw data per bunch crossing; however, full reconstruction of all collision events is not feasible with existing computing resources necessitating the use of a trigger system.

At the LHC, events of interest are selected using a two-tiered trigger system [1, 2]. The first level (L1), composed of custom hardware processors, uses information from the calorimeters and muon detectors to select events at a rate of around 100 kHz within a time interval of 2–4  $\mu\text{s}$ . The second level, known as the high-level trigger (HLT), consists of a farm of processors running a version of the full event reconstruction software optimized for fast processing, and reduces the event rate to around 1 kHz before data storage.

To make a trigger decision for each event, the HLT performs a real-time (online) physics object reconstruction and applies a selection based on the characteristics of the reconstructed objects. The full HLT algorithm is a collection of independent trigger paths, each intended to serve a different event selection purpose. Trigger paths consist of sequences of producer modules, which build collections of objects; and filter modules, which reject events that do not fulfill certain criteria. Most trigger paths contain multiple phases of reconstruction and filtering, and generally the later phases of reconstruction yield physics objects whose performance is closer to that of their offline counterparts. If an event is accepted by the final filter of any trigger path, it is accepted by the HLT.

A number of factors restrict the trigger rates that the HLT can achieve:

---

\*e-mail: [jduarte1@fnal.gov](mailto:jduarte1@fnal.gov)

- The amount of data storage space and the maximum throughput of the data acquisition system (DAQ)
- The capacity of the prompt reconstruction system
- HLT computing resources, which limit the complexity of the online reconstruction

Data parking in CMS, or delayed stream in ATLAS, in which selected events are saved directly to tape with no prompt reconstruction, has also been used in past LHC runs to increase the amount of data collected. While this strategy circumvents the restriction on rates imposed by the offline reconstruction system, it is limited by the other factors listed above.

In this note, we describe data scouting, a technique that leverages online reconstruction of physics objects in order to attain extremely high trigger rates. Scouting complements data parking by providing new opportunities for physics analysis outside the boundaries of the traditional trigger strategy.

Data scouting was first introduced by the CMS collaboration in 2011 [3–6]. The LHCb and ATLAS collaborations implemented similar data-taking streams for LHC Run 2 [7–9].

## 2 Data scouting: an alternative trigger paradigm

The aim of data scouting is to record physics events at the highest possible rate while providing physics objects whose performance is suitable for offline analysis. To do this, LHC experiments take advantage of the online reconstruction algorithms. Trigger-level physics objects are slightly less performant than their offline counterparts, but for certain analyses, the difference does not significantly affect the sensitivity. Saving only the trigger-level objects instead of the full raw detector data makes the throughput and the size on disk much smaller.

The data scouting strategy is implemented via dedicated streams at the HLT. Each data scouting stream contains a number of trigger paths (scouting triggers), which perform event reconstruction and selection in the same way as standard HLT paths. However, the selection criteria are much looser than for standard paths and thus the rate of events passing the selection is much greater.

For events passing one or more scouting triggers, additional online reconstruction sequences are run in order to produce all physics objects necessary for an offline measurement or search. The produced objects are converted to a special compact event format and saved to disk. The data recorded by scouting triggers is made available offline and can be used for physics analysis. For these events, no offline reconstruction is performed, and the raw data is not saved.

The scouting approach has the following advantages over the standard trigger strategy:

- The reduced, compact event format requires negligible space on disk and does not place any additional strain on the DAQ system. Events are 100 to 1000 times smaller on disk than the standard raw data format.
- No offline reconstruction is required; all reconstruction is performed online
- Scouting trigger paths can run ‘in the shadow’ of standard HLT paths, saving physics objects, reconstructed by the standard HLT paths even for events that are rejected by those paths

Scouting has been used to increase the total number of LHC events recorded for physics by a factor of 2–6 beyond what the standard trigger strategy provides.

### 3 Data scouting in CMS

The first scouting trigger was deployed at the CMS HLT during the last few proton-proton fills of the 2011 LHC run. The trigger and associated stream collected data equal to  $0.13 \text{ fb}^{-1}$ . Events with  $H_T$  (defined as the scalar sum of jet transverse momenta) larger than 350 GeV were recorded and saved in a reduced format, containing only the set of anti- $k_r$ ,  $R = 0.5$  jets [10, 11] reconstructed from particle-flow (PF) candidates by the HLT. The data were used to perform a search for heavy resonances decaying to dijets [4]. The search demonstrated sensitivity to resonances with masses between 0.6 and 0.9 TeV, a parameter region inaccessible to the standard CMS dijet resonance search.

Subsequently, the strategy was repeated for the full 2012 CMS dataset, lowering the scouting trigger selection to  $H_T > 250 \text{ GeV}$  to accommodate an even larger rate of events. Due to CPU concerns related to the high rate, calorimeter jets were reconstructed and saved instead of PF jets. The collected data, corresponding to  $18.8 \text{ fb}^{-1}$ , were used to perform another dijet resonance search [12], whose results were interpreted as limits on the mass and coupling of a hypothetical leptophobic  $Z'$  resonance decaying to quarks.

In Run 2, the data scouting strategy was expanded, with an aim to maintain the ability to search very low in  $H_T$  using calorimeter jets, while also providing an event format capable of supporting a broader range of scouting analyses. Two streams were deployed at the HLT for data taking in 2015–2018: one saving an event content based on calorimeter jets (the calo-scouting stream) and one saving an event content based on particle-flow (PF) jets (the PF-scouting stream). The PF algorithm [13] aims to reconstruct and identify each individual particle in an event, with an optimized combination of information from the various elements of the CMS detector. The PF jet energy resolution amounts typically to 15% at 10 GeV, 8% at 100 GeV, and 4% at 1 TeV, to be compared to about 40%, 12%, and 5% for calorimeter jets. In order to run the PF algorithm online within the allotted CPU time of around 200 ms, a speed-optimized configuration of the full CMS track reconstruction is used [14].

Finally, new dedicated scouting event formats were developed, featuring a set of minimalist C++ objects to store scouting physics objects as vectors of basic data types, ensuring low overhead and forward compatibility with future versions of CMS software.

#### 3.1 Calo and PF-scouting streams

Triggers in the calo-scouting stream reconstruct jets from calorimeter deposits and the main signal trigger requires  $H_T > 250 \text{ GeV}$ . The event content for this stream includes the reconstructed calorimeter jets, the missing transverse momentum (MET), and  $\rho$ , a measure of the average energy density in the event, as depicted in Fig. 1. Local pixel track reconstruction provides b-tagging information for the jets. The size of this event content is about 1.5–3 kB on average.

Similarly, triggers in the PF-scouting stream run the online version of the full PF sequence to reconstruct selected events and the main signal trigger selects events with  $H_T > 410 \text{ GeV}$ . Additionally, the stream contains a trigger path selecting events with two muons having invariant mass above 3 GeV, both with and without a primary vertex constraint, allowing the possibility of searches for prompt and displaced dimuon resonances. The event content for this stream includes the reconstructed PF jets, the PF MET, the average energy density in the event  $\rho$ , a collection of primary vertices, and all PF candidates with  $p_T > 0.6 \text{ GeV}$ . It also contains electron, muon, and photon objects, as depicted in Fig. 1. The size of this event content is approximately 10–15 kB per event on average.

Auxiliary prescaled trigger paths are also included both in calo and PF streams in order to facilitate measurements of the signal trigger efficiency. For example, the measured trigger efficiency of the calo-scouting stream as a function of dijet invariant mass is shown in Fig. 2.

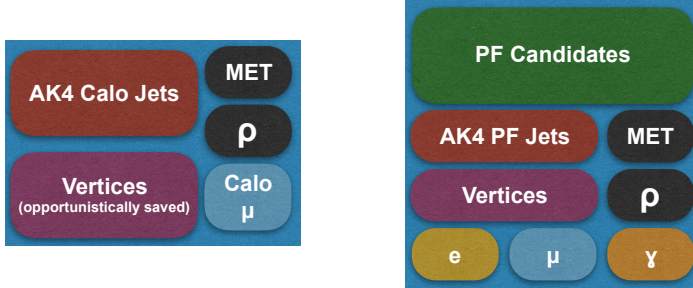


**Figure 1.** Calo and PF-scouting event content. The corresponding sizes per event are approximately 1.5–3 kB and 10–15 kB, respectively

Data stream	Rate at $10^{34} \text{ cm}^{-2} \text{ sec}^{-1}$	Bandwidth (MB/s)
Calo-scouting $H_T$ signal	3700	11
PF-scouting $H_T$ signal	720	9
PF-scouting dimuon signal	480	6
Commissioning (PF + Calo)	30	<1
Monitoring	26	23

**Table 1.** CMS rates and bandwidths measured in 2016 data for various scouting data streams. The row marked ‘Commissioning (PF + Calo)’ represents all auxiliary (non-signal) trigger paths in either the calo-scouting or PF-scouting streams.

### 3.2 Monitoring stream

To facilitate comparisons of the online physics objects to their offline reconstructed counterparts, and to use the CMS Data Quality Monitoring (DQM) framework to monitor the scouting data, a separate monitoring stream was deployed. This stream contains prescaled versions of all scouting triggers in the calo-scouting and PF-scouting streams. Events selected for this stream are both saved in the reduced scouting event format and sent to the CMS prompt reconstruction system for offline processing, which enables detailed object-by-object comparisons of the online and offline performance. Representative rates and bandwidths for all CMS scouting and monitoring streams in 2016 are shown in Tab. 1.

## 4 Trigger-object-level object analysis in ATLAS and turbo stream in LHCb

In ATLAS, the trigger-object-level analysis (TLA) approach allows jet events to be recorded at a peak rate of up to twice the total rate of events using the standard approach, while using

less than 1% of the total trigger bandwidth [15]. The HLT reconstructs anti- $k_t$   $R = 0.4$  jets from groups of contiguous calorimeter cells (topological clusters), in which each cell’s inclusion is based on the significance of its energy deposit over calorimeter noise [16]. Trigger-level jets with  $p_T > 20$  GeV are stored, including a set of calorimeter variables characterizing the jet [17], such as information about the jet quality and structure. The size of these events is less than 0.5% of the size of full events. All events containing at least one L1 jet with  $E_T > 100$  GeV are selected and recorded in the 2016 dataset. The gain in recorded events from ATLAS TLA is shown in Fig. 2.

At the beginning of LHC Run 2, LHCb, with its upgraded computing infrastructure and a more efficient use of the Event Filter Farm (EFF) storage of 5.2 PB, began providing resources for an online reconstruction with a similar quality to that of the offline reconstruction. This is achieved through real-time automated calculation of the final calibrations of the sub-detectors. In the *turbo stream*, a compact event record is written directly from the trigger and is prepared for physics analysis by the Tesla application. Using the turbo stream, LHCb was able to record  $J/\psi \rightarrow \mu^+\mu^-$  candidates with invariant masses  $m(\mu^+\mu^-)$  within 150 MeV of the known value and measure the forward  $J/\psi$  production cross section [18]. The LHCb turbo stream was also used to measure prompt charm production cross sections [19].

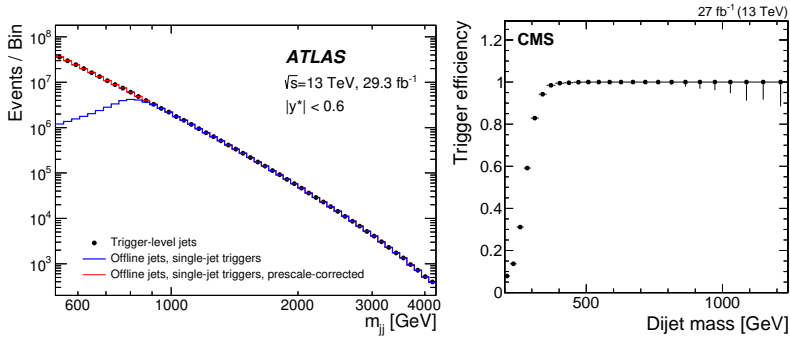


**Figure 2.** Comparison between event acceptance for offline jets and trigger-level jets for ATLAS (left) and calo-scouting trigger efficiency for CMS (right).

## 5 Dijet resonance searches in CMS and ATLAS

CMS data collected in the calo-scouting stream in 2012 and 2016 were used to perform searches for dijet resonances with masses in the range 0.5–1.6 [12] and 0.6–1.6 TeV [20], respectively. The 2016 search was carried out with  $27 \text{ fb}^{-1}$  of pp collision events<sup>1</sup> satisfying the  $H_T > 250$  GeV trigger requirement. Geometrically close anti- $k_t$   $R = 0.4$  jets are combined into two “wide jets” with a jet radius of  $R = 1.1$  and the dijet invariant mass is required to be  $m_{jj} > 0.49$  TeV. Background from  $t$ -channel dijet events is suppressed by requiring  $|\delta\eta_{jj}| < 1.3$ .

The jet energy scale of the HLT calorimeter jets was calibrated to be the same as the jet energy scale of the offline PF jets using the monitoring dataset and a dijet balance “tag-and-probe” method [21].

Fig. 3 shows the parametric fits to the scouting dijet mass spectra in both 2012 and 2016.

<sup>1</sup>The L1  $H_T$  triggers suffered an inefficiency in  $9 \text{ fb}^{-1}$  of data at the end of the run.

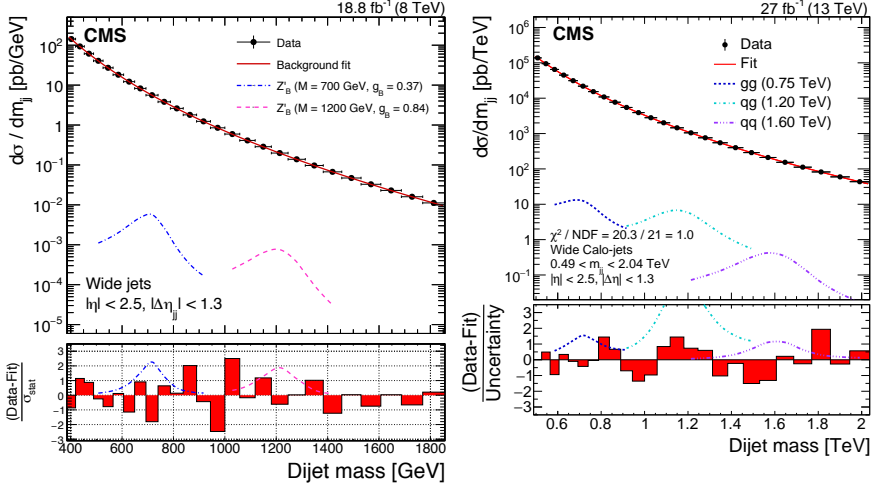


**Figure 3.** Parametric fits of CMS low-mass calo-scouting 2012 data (left) [12] and 2016 data (right) [20].

The analogous dijet search in ATLAS used  $29.3 \text{ fb}^{-1}$  of 2015 and 2016 data and required at least two trigger-level jets with leading (subleading)  $p_T > 220$  (85) GeV and  $|\eta| < 2.8$ . The analysis search for dijet resonances with a masses between 450 GeV and 1800 GeV. To search for resonances with  $700 < m_{jj} < 1800$  GeV, events are required to have  $|y^*| < 0.6$ , where  $y^* = (y_1 - y_2)/2$  and  $y_1$  and  $y_2$  are the rapidities<sup>2</sup> of the highest- and second-highest- $p_T$  trigger-level jets. To search for lower-mass resonances, with  $m_{jj} > 450$  GeV, events with  $|y^*| < 0.3$  are selected from the 2015 data sample.

The trigger-level jet energy and direction are corrected to those of simulated particle-level jets built from stable particles, excluding muons and neutrinos. The custom calibration recipe includes the standard calibrations applied to offline jets as well as any residual difference between trigger-level jets and offline jets is accounted for in a dedicated trigger-to-offline correction, based on the  $p_T$  response and derived from data in bins of jet  $\eta$  and  $p_T$ . After the full calibration procedure, the energy of trigger-level jets is equivalent to that of offline jets to better than 0.05% for invariant masses of 400 GeV.

Finally, the SM background distribution is determined using a sliding-window fit [22] as shown in Fig. 4.

Upper limits on the coupling as a function of mass for a model of a leptophobic  $Z'$  resonance with a universal quark coupling,  $g'_q$  [23–25] are derived for both analyses. The interaction Lagrangian for this model is

$$\mathcal{L}_{Z'} = \sum_q g'_q Z'_\mu \bar{q} \gamma^\mu q. \quad (1)$$

A summary of the constraints from these searches as well as others is shown in Fig. 5. In particular, the impact of the scouting and trigger-level analyses on the  $g'_q$  sensitivity can be seen for masses between 0.45 and 1 TeV. Over this mass range, the sensitivity to the coupling to the universal quark coupling is improved by a factor of two or more compared to pre-LHC searches.

<sup>2</sup>The rapidity,  $y$ , is defined as  $\frac{1}{2} \log[(E + p_z)/(E - p_z)]$

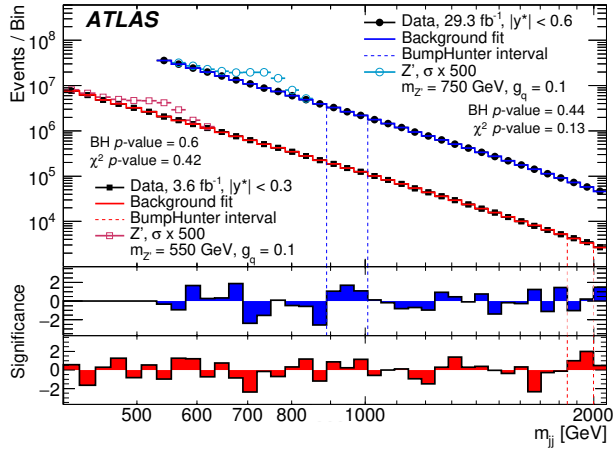


Figure 4. Sliding window fits of ATLAS trigger-object-level analysis in 2015 and 2016 data [9].

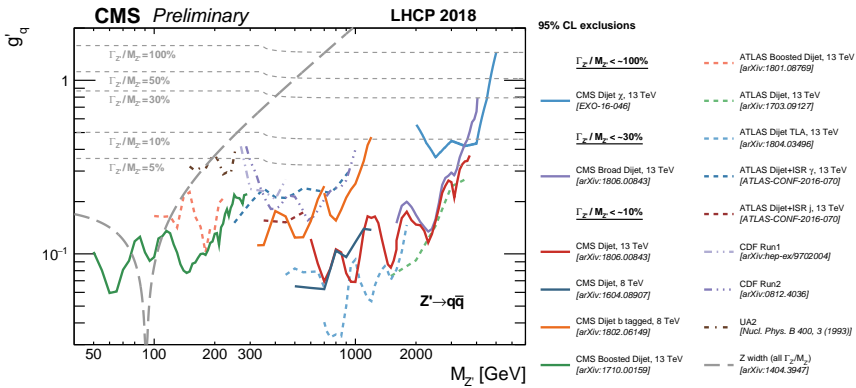


Figure 5. Summary of 95% CL upper bounds on the universal quark coupling for a leptophobic  $Z'$  mediator.

## 6 Summary

Data scouting allows physics events to be collected at a rate dramatically higher than what is nominally achievable with the standard LHC trigger systems. It is implemented with no changes needed to the basic software-based high-level-trigger infrastructure and does not place an additional strain on the DAQ, disk resources, or the reconstruction system.

In CMS, the two scouting streams deployed for Run 2 of the LHC strike a balance between specialization and versatility, with one stream oriented towards dijet resonance searches and the other designed to support arbitrary searches based on hadronic final states. The first physics results using the LHC Run 2 data scouting have been published from CMS, ATLAS, and LHCb, and it is hoped that analyzers will take full advantage of this tool to search in other previously unexplored regions at the LHC.

## References

- [1] V. Khachatryan et al. (CMS), JINST **12**, P01020 (2017), 1609.02366
- [2] A. Ruiz-Martinez, A. Collaboration, Tech. Rep. ATL-DAQ-PROC-2016-003, CERN, Geneva (2016), <https://cds.cern.ch/record/2133909>
- [3] Tech. rep. (2012), <https://cds.cern.ch/record/1480607>
- [4] Tech. Rep. CMS-PAS-EXO-11-094, CERN, Geneva (2012), <https://cds.cern.ch/record/1461223>
- [5] D. Anderson (CMS), *Data Scouting in CMS*, in *Proceedings, 38th International Conference on High Energy Physics (ICHEP 2016): Chicago, IL, USA, August 3-10, 2016* (2016), Vol. ICHEP2016, p. 190
- [6] S. Mukherjee (CMS), *Data Scouting : A New Trigger Paradigm*, in *5th Large Hadron Collider Physics Conference (LHCP 2017) Shanghai, China, May 15-20, 2017* (2017), 1708.06925, <https://inspirehep.net/record/1618341/files/arXiv:1708.06925.pdf>
- [7] R. Aaij et al., Comput. Phys. Commun. **208**, 35 (2016), 1604.05596
- [8] Tech. Rep. ATLAS-CONF-2016-030, CERN, Geneva (2016), <http://cds.cern.ch/record/2161135>
- [9] M. Aaboud et al. (ATLAS) (2018), 1804.03496
- [10] M. Cacciari, G.P. Salam, G. Soyez, JHEP **04**, 063 (2008), 0802.1189
- [11] M. Cacciari, G.P. Salam, G. Soyez, Eur. Phys. J. C **72**, 1896 (2012), 1111.6097
- [12] V. Khachatryan et al. (CMS), Phys. Rev. Lett. **117**, 031802 (2016), 1604.08907
- [13] A.M. Sirunyan et al. (CMS), JINST **12**, P10003 (2017), 1706.04965
- [14] M. Tosi, Nuclear and Particle Physics Proceedings **273-275**, 2494 (2016), 37th International Conference on High Energy Physics (ICHEP)
- [15] M. Aaboud et al. (ATLAS), Eur. Phys. J. **C77**, 317 (2017), 1611.09661
- [16] G. Aad et al. (ATLAS), Eur. Phys. J. **C77**, 490 (2017), 1603.02934
- [17] Tech. Rep. ATLAS-CONF-2015-029, CERN, Geneva (2015), <http://cds.cern.ch/record/2037702>
- [18] R. Aaij et al. (LHCb), JHEP **10**, 172 (2015), [Erratum: JHEP05,063(2017)], 1509.00771
- [19] R. Aaij et al. (LHCb), JHEP **03**, 159 (2016), [Erratum: JHEP05,074(2017)], 1510.01707
- [20] A.M. Sirunyan et al. (CMS) (2018), 1806.00843
- [21] V. Khachatryan et al. (CMS), JINST **12**, P02014 (2017), 1607.03663
- [22] M. Aaboud et al. (ATLAS), Phys. Rev. **D96**, 052004 (2017), 1703.09127
- [23] B.A. Dobrescu, F. Yu, Phys. Rev. **D88**, 035021 (2013), [Erratum: Phys. Rev.D90,no.7,079901(2014)], 1306.2629
- [24] Abercrombie et al. (2015), 1507.00966
- [25] G. Busoni et al. (2016), 1603.04156